Cavity-based nondestructive detection of photoassociation in a dark magneto-optical trap

V. I. Gokul, Arun Bahuleyan, S. P. Dinesh, V. R. Thakar, and S. A. Rangwala
Raman Research Institute, C. V. Raman Avenue, Sadashivanagar, Bangalore 560080, India

(Received 29 November 2023; accepted 2 May 2024; published 16 May 2024)

The photoassociation (PA) of a rubidium dimer in a dark magneto-optical trap (MOT) is studied using atom-cavity collective strong coupling. This allows nondestructive detection of the molecule formation process as well as rapid and repeated interrogation of the atom-molecule system. The vacuum Rabi splitting (VRS) measurements from the bright MOT are carefully calibrated against equivalent measurements with fluorescence. Further loading rates in the dark MOT are determined using VRS. This method provides a reliable, fast, and nondestructive detection scheme for detecting the PA using the free atoms coupled to a cavity when the atoms are in a nonfluorescing state.

DOI: 10.1103/PhysRevA.109.053713

I. INTRODUCTION

The detection of multiparticle interaction is a challenging experimental problem. In an ensemble, this can be done by detecting the postcollision product or by interrogating individual participants. This method only allows partial information about the process of interest. For atomic systems, cavity-based measurements are very precise for studying atom-field interactions. In this paper, we adapt the cavity QED technique to detect the photoassociation (PA) of atoms. We aim to demonstrate the power of a cavity-based technique with PA as a representative example, though this technique has wider application, for instance, collision rate measurement between the two overlapping ensembles in the cavity mode volume. PA results when two free atoms in a scattering state absorb one photon and form a bound, excited molecule [1,2] (Fig. 1). The absorbed photon is resonant with the free-to-bound transition, and the excited-state molecule can subsequently decay into free atoms by emitting a photon (Γ_f) or into a bound, ground-state molecule in one of many possible rovibrational states (Γ_b). PA is efficient in an ensemble of ultracold atoms, where the energy of the scattering state is well defined, favoring resonant excitation by a single, narrowband laser. Suitable conditions for PA, therefore, require trapped atoms in magneto-optical traps (MOTs) [3–8], magnetic traps [9,10], or dipole traps [11–13].

Detection of PA in a bright MOT (where the MOT is observable in fluorescence) is done by measuring the resonant loss of the fluorescing atoms. Fluorescence detection is not an option in a dark MOT [14] or for other dark traps. Here, resonant multiphoton ionization (ReMPI) of the resulting ground-state molecule and the subsequent detection of the molecular ion are the main detection tools available [9,15–18]. ReMPI has limited efficiency principally because the ground-state molecules produced by PA are created in various states due to spontaneous emission from the excited state.

In this paper, we present cavity-based, nondestructive detection of the atoms, which are collectively strongly coupled to a low finesse cavity, during PA. In the experiment, we probe the vacuum Rabi splitting (VRS) of the atoms coupled to the cavity [19,20]. As will be shown below, the technique works very well for a dark MOT, where atomic fluorescence is not detectable. In addition, this measurement is nondestructive, as it probes the atoms and not the molecules, with very low light intensity detuned with respect to the atomic resonance, resulting in no additional loss of atoms from the trap. This combination of properties allows for continuous monitoring of PA, which we demonstrate so that its temporal evolution can also be measured and studied. Below, we first explain our experimental setup, calibrate our technique with a bright MOT, demonstrate results with the dark MOT, discuss the different ratios of bright and dark MOT resonance intensities, and conclude with some applications of this method. Our technique complements the recent direct strong-coupling signature of PA [21] observed in a high-finesse ($F \approx 5 \times 10^4$) cavity. Even though the finesse in our experiment does not allow for a direct strong-coupling signature of PA, detecting atoms instead of molecules allows us to detect PA and calculate rates. A relatively low finesse (≈ 330) cavity used in the experiment implies that one can perform these measurements even by having a cavity outside the vacuum.

II. EXPERIMENTAL SETUP

The experimental setup consists of a Fabry-Pérot (FP) cavity cocentered with a dilute gas of ultracold ^{85}Rb atoms that are trapped in an MOT. A detailed overview of the experimental setup is discussed in previous work [22,23]. The FP cavity has length $L \cong 45.7$ mm, finesse $F \approx 330$, and linewidth $\kappa \approx 4.4$ MHz. A cooling beam detuned -12 MHz from $F = 3$ to $F' = 4$ and repumper on $F = 2$ to $F' = 3$ form the bright MOT. The dark MOT is implemented by obstructing the center of an independent repumper beam with a ≈2-mm disk shelving the atoms in the $F = 2$ nonfluorescing state. A double pass acousto-optic modulator (AOM) is used to switch both repumping lasers, allowing us to change between bright and dark MOTs in our system. Additionally, a weak depumping beam ($\approx 1\,\mu$W) from $F = 3$ to $F' = 3$ is used to maximize dark MOT density. For a cooling power of 25 mW and repumping power of 3.5 mW the measured peak density

of the dark MOT $\rho_0 \approx 1.7 \times 10^{10}$ cm^{-3}. For all dark MOT measurements, the cavity is referenced to the $F = 2$ to $F' = 3$ transition [24], and a weak probe beam is scanned across the same transition. The cavity output is monitored using a photomultiplier tube and a charge-coupled device camera. A separate free-space setup is used to collect MOT fluorescence [23]. The PA beam has ≈2-mm diameter and is incident perpendicular to the cavity axis. The wavelength of this PA laser is continuously monitored using a wavemeter.

In the experiment, κ and excited-state decay (Γ) are much greater than single atom-cavity coupling constant $g_0 = \sqrt{\mu_{23}^2 \omega_{23}/2\hbar\epsilon_0 V_c} \approx 0.141$ MHz for the $F = 2 \rightarrow F' = 3$ transition [25], where μ_{23} is the transition dipole matrix element for the probe transition and V_c is the cavity mode volume. So, while a single atom cannot couple strongly to the cavity [19,26] when N_c atoms are present in V_c, each of these atoms can couple to a single cavity photon, resulting in an effective coupling strength of $g_N = g_0\sqrt{N_c}$ [19,27–29]. In this collective strong-coupling regime, the condition for observing strong-coupling effects becomes $g_N = g_0\sqrt{N_c} \gg \Gamma, \kappa$. For a MOT with density distribution $\rho(x, y, z)$ co-centered with a cavity mode, N_c can be calculated using $N_c = \int \rho(x, y, z)|\psi(x, y, z)|^2 dV$, where ψ is the cavity mode function [23].

For our experimental parameters, atom numbers as low as $N_c \gtrsim 1000$ can be measured via VRS in a collective strong-coupling regime. Since the separation between VRS peaks is given by $2g_0\sqrt{N_c}$, any change in VRS corresponds to a change in N_c, which is a direct measure of change in MOT atom number [29]. This allows detection of PA transitions in the dark MOT using VRS.

III. RESULTS

A. PA resonances and loading rates in a bright MOT

The potential-energy curves for the long-range photoassociated Rb_2 [30,31] molecule in the D_2 transition are shown in Fig. 1. From the selection rule the only transitions relevant and observed in our experiments are 0_g^-, 0_g^+, and 1_g [32]. In the presence of a PA laser, two ground-state Rb atoms can form a weakly bound excited-state Rb_2 molecule (0_g^-, 0_g^+, or 1_g). This excited-state molecule decays back into a high vibrational ground-state molecule ($^1\Sigma_g^+$ or $^3\Sigma_u^+$) or two free atoms by photoemission.

In the experiment, the bright MOT has a peak density of ≈8×10^{10} cm^{-3} and full width at half maximum of ≈180 μm. The PA laser is tuned from 12 814 to 12 816 cm^{-1} and six prominent PA resonances are addressed. These transitions are labeled as PA1–PA6. The peak intensity of the PA laser is ≈15 W/cm^2, which is sufficient to saturate the PA transition. Figure 1(b) shows the trap-loss measurement for these PA transitions. The dashed lines in the figure represent the closest calculated vibrational level for the excited-state *ab initio* molecular potentials [31]. As this method is nondestructive, one can perform continuous measurements to study the evolution and dynamics of the system. As proof of principle, we measure the loading rates in the MOT using VRS and calculate loss rates in the system during PA.

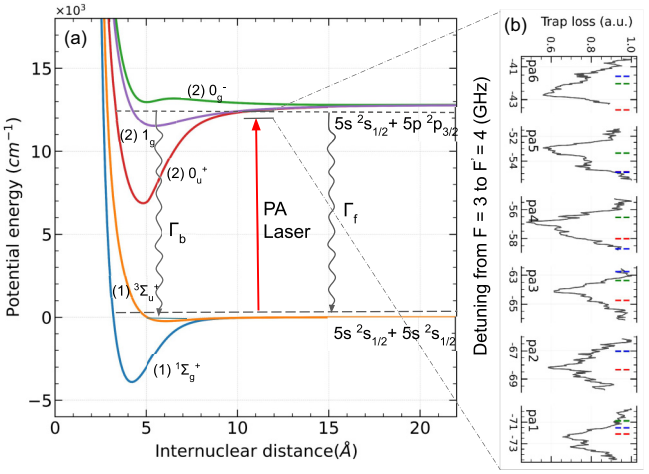

FIG. 1. Potential-energy curves for the Rb_2 molecule relevant in the experiment and various transitions. (b) Trap-loss spectrum for different PA transitions in the bright MOT. Here, PA frequency is referenced to the $F = 3$ to $F' = 4$ D_2 transition of Rb.

The MOT fluorescence with a bright MOT provides a direct calibration of the VRS detection. As bright MOT atoms are predominantly in the $F = 3$ state, the cavity is locked to the $F = 3$ to $F' = 3$ transition, and the probe is scanned across the same transition. For this measurement, use the value of $\tilde{g_0} = \sqrt{\mu_{33}^2 \omega_{33}/2\hbar\epsilon_0 V_c} \approx 0.13$ MHz. The frequency of the PA transition is monitored by a wavemeter. Change in the VRS signal is observed in addition to the trap-loss fluorescence signal on PA resonances. The ground-state molecules and the majority of the free atoms formed from excited-state molecules during a PA are not trapped in a MOT [33], resulting in a reduction of atom number in the MOT. This results in a smaller VRS when the PA laser is resonant to any of the transitions. This reduction in VRS measures the formation of excited-state Rb_2 molecules by PA.

As shown in Fig. 2, a direct measure of the loading curve using VRS is also performed for the bright MOT with the PA laser kept off and on transition. Here, the probe laser is scanned at a rate of 8 Hz for 10 s and frequency is referenced with respect to saturated absorption spectroscopy (SAS). The MOT coil is turned off for a short time, and the probe output is continuously monitored. As a result, once the MOT starts to load, rapid VRS measurements are possible. The VRS signal is fitted with an intracavity intensity function for a two-level atom coupled to a cavity given by the Jaynes-Cumming model to extract N_c (see Appendixes). The photomultiplier value when the probe is far-detuned to the atomic transition is subtracted from the signal for background reduction. A possible source of noise in the background is from the hybrid trap geometry of the experimental apparatus [34] resulting in small scattering from ion-trap wires for high-intensity PA beams. This background is reduced by adjusting the angle and size of the PA beam. The loading rate is calculated from the VRS signal. Figure 2(a) shows the evolution of VRS as the MOT loads. Initially, when there are no atoms in the MOT, the cavity transmission corresponds to an empty cavity transmission. As

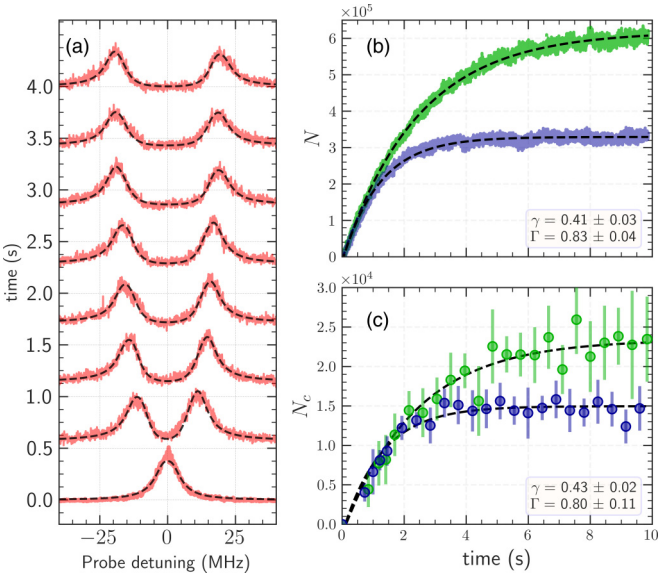

FIG. 2. Loading curve for the bright MOT: (a) time evolution of VRS as the MOT loads and (b) loading curve from MOT fluorescence. Here, the green curve is when PA is off-resonant, and the blue curve is when PA is on-resonance. The loading rate Γ and γ are calculated from the fit. (c) Loading curve measured from VRS. Each point is an average of five repeated measurements and the error bar is the standard deviation. All the measurements are done on the PA5 transition.

the MOT builds up, the number of atoms in the cavity mode increases, resulting in an increase in VRS.

Figure 2(b) shows the MOT loading from fluorescence when the PA laser is kept on-resonance (blue) and off-resonance (green). This is fitted with $N(t) = N_0[1 - \exp(-\Gamma t)]$ (see Appendixes) to extract the loading rate (Γ). The loading rates are given in Table I. The loss rate in the MOT due to PA is therefore $\gamma_{\rm PA} = \Gamma - \gamma = 0.42 \pm 0.07\ {\rm s}^{-1}$. Figure 2(c) shows the same loading measured using VRS with on-resonant (blue circle) and off-resonant (green circle) PA. The loss rate in the MOT calculated from VRS is $\gamma_{\rm PA} = 0.37 \pm 0.13\ {\rm s}^{-1}$. These values agree very well with MOT fluorescence measurement, validating VRS-based measurements. The error bar in the VRS is mostly from the fluctuation of N_c. The σ of the MOT in our experiment is ≈80 μm, and the beam waist for the $\rm TEM_{00}$ mode is $\omega_0 \approx 78$ μm. As a result, any slight fluctuation in the MOT causes a change in N_c. In the present experiment, this is compounded by the fact that the atom-cavity system is within an ion trap, the electrodes of which scatter some fraction of MOT light, increasing the fluctuations [34]. The ion trap is formed by four 80-μm tungsten wires separated by 1.5, 3, and 1.5 mm, respectively, in a modified spherical Paul trap geometry. These ion trap wires cause regions of unequal intensity in the MOT beam, which has a size of 10 mm. This is the inherent cause of fluctuations in the MOT and, thereby, N_c in Figs. 2 and 3.

TABLE I. Loading rates calculated from the fit for the PA laser kept on and off transition. Columns represent measurements using fluorescence and VRS.

	Fluorescence	VRS
$\rm PA_{OFF}$ (γ)	0.41 ± 0.03	0.43 ± 0.02
$\rm PA_{ON}$ (Γ)	0.83 ± 0.04	0.80 ± 0.11

B. PA resonances and loading rates in a dark MOT

In systems like dark MOTs, most of the atoms are in the nonfluorescing state ($F = 2$). As a result, a direct fluorescence trap-loss signal for PA resonances is not possible. The VRS measurement makes such detection possible even when the system is in a dark state. For this detection, the cavity is locked to the $F = 2$ to $F' = 3$ transition. A weak probe laser is scanned across the same transition and referenced to SAS. Since the atoms are in the $F = 2$ state, all the PA resonances (PA1–PA6) are shifted by ≈3.03 GHz, which is the difference in frequency between $F = 2$ and 3 hyperfine levels. The PA laser with peak intensity ≈15 $\rm W/cm^2$ is incident on the dark MOT. The cavity transmission is monitored with PA kept on- and off-resonant for all six transitions.

Figures 3(a)–3(f) show the change in VRS signal when the PA laser is on-resonance (blue) and off-resonance (green) for all the transitions. In all cases, the blue curve is shifted for better visibility. The values of all VRS and corresponding molecular transitions are given in Table I. As seen from Fig. 3 the value of VRS decreases when a PA transition is addressed, which is a direct measurement of the formation of the $\rm Rb_2^*$ molecule due to PA in a dark MOT. The slight asymmetry in the VRS peak for PA5 and PA6 is likely due to the small scattered repumper light in the dark MOT, causing a driven VRS signal for low atom numbers when the value of $g_0\sqrt{N_c}$ is small. Since the scattered light intensity is relatively low, the value of N_c calculated from this split will be within the error bar from N_c calculated for a nondriven case.

To demonstrate the time evolution capabilities, the loading rates for the dark MOT are measured in the presence of the PA. For this measurement, the probe laser is locked to the $F = 2$ to $F' = 3$ transition using SAS. This locked laser is passed through two double-pass AOMs. One of the AOMs is scanned continuously at a rate of 4 Hz for 20 s. For this loading measurement, peak intensity of the PA laser was kept at ≈10 $\rm W/cm^2$. Figure 3(g) shows the N_c as a function of time when the PA laser is kept off-resonance (green circle) and on-resonance (blue circle). The loading rate of the dark MOT on-resonance $\Gamma_D = \gamma_D + \gamma_{{\rm PA},D} = 0.33 \pm 0.06\ {\rm s}^{-1}$, where $\gamma_D = 0.13 \pm 0.03\ {\rm s}^{-1}$, for PA5, as shown in Fig. 3(g). From this, the loss rate in the dark MOT due to PA is calculated as $\gamma_{{\rm PA},D} = 0.20 \pm 0.09\ {\rm s}^{-1}$. Figure 3(h) shows the ratio of N_c when PA is on- and off-resonant to the transition as a function of PA laser intensity. As the PA intensity increases, the fraction of atoms getting converted to the PA molecule increases, showing a reduction in the ratio of the N_c value. The dashed line, which is a linear fit, shows good agreement for lower PA intensity to theoretical expectation. For higher intensities, the saturation effect results in deviation from the linear fit. This saturation in PA rate for higher PA intensity is well known both theoretically [35] and experimentally [10,36,37]. The PA rate depends on the

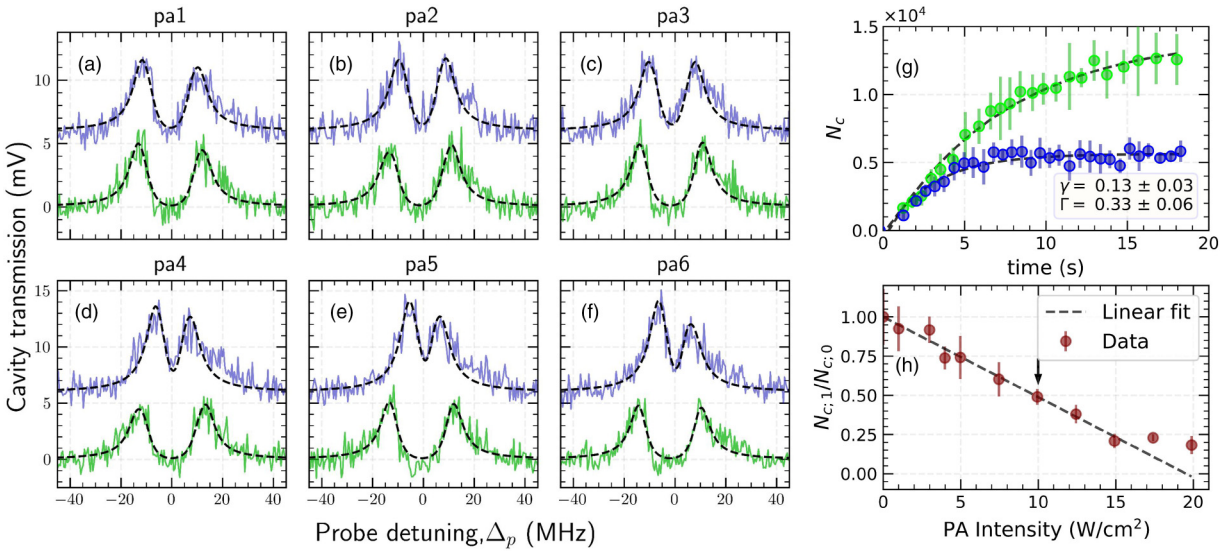

FIG. 3. Direct detection of PA resonances in the dark MOT using VRS. (a–f) Change in VRS for various PA resonances. The blue line is when the PA laser is kept on-resonance, and the green plot is when the PA laser is kept off-resonant. The figure shows the VRS for a single sweep and the theoretical fit of the data to determine the peak separation. (g) Loading curve using atoms coupled to the cavity mode (N_c). Here, the green circle is when the PA laser is kept off-resonant to the transition, and the blue circle is when the PA laser is kept on-resonant. (h) The ratio of N_c when the PA laser is on-transition ($N_{c,1}$) to off-transition ($N_{c,0}$) as a function of PA intensity. The arrow represents the peak intensity used for dark MOT loading measurements. Each point is an average of five measurements. All the measurements are done on the PA5 transition.

overlap of scattering wave functions of colliding free atoms and the bound, excited-state rovibrational wave function of their molecular state. The saturation effect in the PA rate is due to the quantum-mechanical unitary limit on the rate of two-body collision.

C. Temperature measurement during PA

A small fraction of atoms that are dissociated from excited molecules can have kinetic energy less than the trap depth. As a result, these atoms do not contribute to the trap-loss signal. However, if they have sufficient energy to increase the average temperature of the MOT [38], an extension of this detection technique is possible. To demonstrate this, temperature measurement using cavity VRS [22] is done for the bright MOT with and without PA. The cavity is locked to the $F = 3 \rightarrow F' = 4$ transition. The probe laser is locked to the same transition, and AOM is scanned at a rate of 2 kHz. MOT beams are switched off using an AOM-based switch for 5 ms. During this period, the MOT expands ballistically, and from the measured value of N_c the standard deviation (σ) of the MOT can be calculated. This gives a direct measure of temperature using the expression [39] $\sigma(\tau)^2 = \sigma_0^2 + \frac{k_B T}{m}\tau^2$. The same procedure is repeated with an on-resonant PA, which is turned off just before the MOT expansion. This ensures that the atoms that are recaptured in the trap contribute to the temperature of the MOT. As shown in Fig. 4, the measured value of temperature of the MOT is $T_{\mathrm{MOT}} = 20.10 \pm 0.66$ μK and with on-resonant PA is $T_{\mathrm{PA}} = 21.86 \pm 1.01$ μK, which shows that the fraction of atoms recaptured by the decay of the excited molecules is negligible.

IV. DISCUSSION AND CONCLUSION

Cavity-based techniques have been used for studying real-time dynamics in atomic systems [40]. Here, we experimentally show the potential of such a scheme for detecting photoassociation in the dark MOT. The advantages of PA from an optically dark ensemble are numerous, the most prominent being the larger fraction of atoms converted to molecules (Fig. 3), since the dark MOT atoms are all in the same ground state. Further, in systems like the dark MOT, the PA rate ($\gamma_{\mathrm{PA},D}$) is larger compared to the loading rate (γ_D), giving a higher fraction of PA (see Appendixes). The cavity-

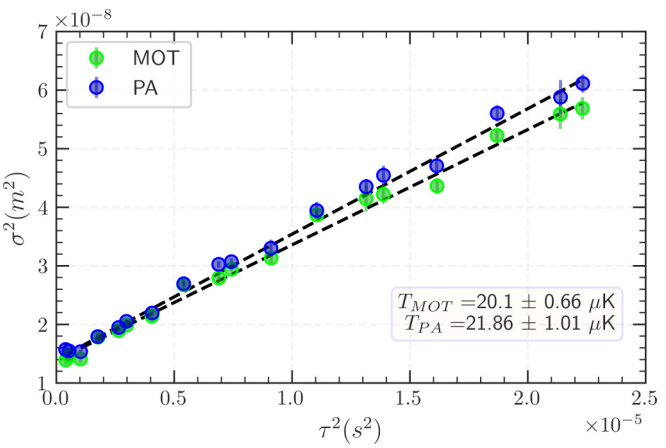

FIG. 4. Temperature measurement during PA. Here, the green circle represents measurement with PA, and the blue circle is without PA. Each data point is an average of five measurements.

based technique of detection, which probes the free atoms instead of the molecules [41,42], can be used very effectively for detection, in scenarios where detection is difficult and in cases like three-particle PA [43] or PA of Rydberg molecules [44] with accuracy.

This technique is expected to be particularly useful where direct fluorescence detection is not possible. As the method is nondestructive by nature, atom-molecule population dynamics in the system can be studied continuously. Since ultracold molecules are not trapped in our experiment, a direct detection of atom-molecule collision was not possible. However, the extension of this method for such experiments is straightforward, making this way of studying interactions more universal. In summary, the present paper demonstrates how cavity techniques can be applied to detect complex processes and yield accurate results in very challenging systems and spatially compact geometries.

ACKNOWLEDGMENTS

The authors would like to thank the Department of Science and Technology and Ministry of Electronics and Information Technology (MeitY), Government of India, under Centre for Excellence in Quantum Technologies Grant No. 4(7)/2020-ITEA.

APPENDIX A: INTRACAVITY INTENSITY OF A TWO-LEVEL SYSTEM COUPLED TO A CAVITY

The rate equation for a two-level system coupled to a cavity is given by [45]

$$\frac{d\alpha}{dt} = -(\kappa_t - i\Delta_{\text{probe cav.}})\alpha - i\sum_{j=1}^{N} g_j\rho_j - \eta,$$
$$\frac{d\rho_j}{dt} = -(\Gamma/2 - i\Delta_{\text{probe at.}})\rho_j + ig_j\alpha(2\rho_{e,j} - 1),$$
$$\frac{d\rho_{e,j}}{dt} = -\Gamma\rho_{e,j} + i(g_j\alpha^*\rho_j - g_j\alpha\rho^*),$$

where $\rho_{e,j}$ is the excited-state population of the jth atom and ρ_j is the coherence between the ground and excited state, η is the fraction of light injected into the cavity, α is the cavity field and g_j is the atom-cavity coupling strength of the jth atom. The detunings of the probe from the atomic transition (ω_a) and cavity transition (ω_{cav}) are given by $\Delta_{\text{probe at.}}$ and $\Delta_{\text{probe cav.}}$, respectively. In steady state, assuming $\omega_{\text{cav}} = \omega_a$ the intracavity intensity is given by

$$|\alpha|^2 = \frac{|\eta|^2\left(\frac{\Gamma^2}{4} + \Delta^2_{\text{probe at.}}\right)}{\left(\frac{\kappa_t\Gamma}{2} - \Delta^2_{\text{probe at.}} + g_t^2\right)^2 + \left(\kappa_t + \frac{\Gamma}{2}\right)^2\Delta^2_{\text{probe at.}}},$$

where $g_t = g_0\sqrt{N_c}$. The VRS data are fitted with $|\alpha_1|^2 + |\alpha_2|^2$ to take into account anharmonicity in the VRS [46].

APPENDIX B: LOADING RATES IN THE MOT

The rate equation for the number of atoms (N) in the trap with the PA laser is given by [36,47]

$$\frac{dN}{dt} = L - \gamma N - (\beta + \beta_{\text{PA}})\int n^2(r)d^3r, \tag{B1}$$

where L is the rate at which atoms are loaded into the trap, γN is the rate at which atoms are lost from the trap due to background collisions, β is the loss rate due to collision with trapped atoms, and β_{PA} is the loss rate due to photoassociation. The dark MOT has a uniform density [23] ($n_{\max}$) inside the trap. As a result, Eq. (B1) can be rewritten as

$$\frac{dN}{dt} = L - [\gamma + (\beta + \beta_{\text{PA}})n_{\max}]N,$$
$$N(t) = N_0[1 - \exp(-\Gamma t)], \tag{B2}$$

where $\Gamma = \gamma + (\beta + \beta_{\text{PA}})n_{\max}$. In steady state,

$$\frac{N_{\text{PA}}}{N_{\text{at}}} = 1 - \frac{\gamma + \beta n_{\max}}{\gamma + (\beta + \beta_{\text{PA}})n_{\max}}, \tag{B3}$$

where N_{at} is the steady-state atom number without PA and N_{PA} is the fraction of atoms converted into PA. Even for a bright MOT with peak density $\rho_0 \approx 8 \times 10^{10}$ cm^{-3} this can be used to find the approximate value of β_{PA} assuming a radiation trap model for MOT density [47].

TABLE II. VRS values for different PA resonances. VRS (off) is when the PA laser is off-resonant, and VRS (on) is when the PA laser is on-resonant.

	Nearest PA resonance	VRS (off) (MHz)	VRS (on) $MHz)
PA1	$0_g^-, v = 50$	25.41	22.53
	$1_g, v = 164$	±0.8	±1.01
	$0_u^+, v = 251$		
PA2	$0_g^-, v = 51$	24.43	20.95
	$1_g, v = 165$	±0.54	±1.44
	$0_u^+, v = 252$		
PA3	$0_g^-, v = 52$	24.82	19.33
	$1_g, v = 166$	±1.141	±1.9
	$0_u^+, v = 253$		
PA4	0_g^-, v=53	22.14	15.18
	$1_g, v = 168$	±1.19	±1.66
	$0_u^+, v = 255$		
PA5	$0_g^-, v = 54$	25.38	12.13
	$1_g, v = 169$	±1.3	±0.58
	$0_u^+, v = 256$		
PA6	$0_g^-, v = 58$	24.28	12.7
	$1_g, v = 173$	±1.32	±0.46
	$0_u^+, v = 260$		

APPENDIX C: PA RESONANCES IN THE DARK MOT

Table II shows the values of VRS measured for different PA transitions in the dark MOT. Here, VRS (off) represents the vacuum Rabi split when the PA laser is kept off-resonance, and VRS (on) is when the PA laser is kept on-resonance. The data are fitted with a theoretical expression for intracavity intensity derived from a two-level atom coupled to a cavity to extract VRS values. Each value given in the table is an average of ten measurements, and the error bar is the standard deviation. As seen from Table II the average value of VRS is always smaller when PA resonance is addressed. The

fraction of excited Rb_2 molecules created can be calculated from $1-(N_{c,1}/N_{c,0}) = 1-(\mathrm{VRS_1}^2/\mathrm{VRS_0}^2)$, where $\mathrm{VRS_1}$ is the split when PA is on-resonance and $\mathrm{VRS_0}$ is the corresponding off-resonance value. All the PA transitions are identified from *ab initio* calculation done in Ref. [31].

[1] H. R. Thorsheim, J. Weiner, and P. S. Julienne, Phys. Rev. Lett. **58**, 2420 (1987).

[2] K. M. Jones, E. Tiesinga, P. D. Lett, and P. S. Julienne, Rev. Mod. Phys. **78**, 483 (2006).

[3] J. Dalibard and C. Cohen-Tannoudji, J. Opt. Soc. Am. B **6**, 2023 (1989).

[4] T. Takekoshi, B. M. Patterson, and R. J. Knize, Phys. Rev. A **59**, R5 (1999).

[5] P. D. Lett, K. Helmerson, W. D. Phillips, L. P. Ratliff, S. L. Rolston, and M. E. Wagshul, Phys. Rev. Lett. **71**, 2200 (1993).

[6] H. Wang, P. L. Gould, and W. C. Stwalley, Phys. Rev. A **53**, R1216 (1996).

[7] A. Fioretti, D. Comparat, C. Drag, C. Amiot, O. Dulieu, F. Masnou-Seeuws, and P. Pillet, Eur. Phys. J. D **5**, 389 (1999).

[8] T. Bergeman, J. Qi, D. Wang, Y. Huang, H. K. Pechkis, E. E. Eyler, P. L. Gould, W. C. Stwalley, R. A. Cline, J. D. Miller, and D. J. Heinzen, J. Phys. B **39**, S813 (2006).

[9] D. Wang, J. Qi, M. F. Stone, O. Nikolayeva, B. Hattaway, S. D. Gensemer, H. Wang, W. T. Zemke, P. L. Gould, E. E. Eyler, and W. C. Stwalley, Eur. Phys. J. D **31**, 165 (2004).

[10] I. D. Prodan, M. Pichler, M. Junker, R. G. Hulet, and J. L. Bohn, Phys. Rev. Lett. **91**, 080402 (2003).

[11] J. D. Miller, R. A. Cline, and D. J. Heinzen, Phys. Rev. Lett. **71**, 2204 (1993).

[12] P. Staanum, S. D. Kraft, J. Lange, R. Wester, and M. Weidemüller, Phys. Rev. Lett. **96**, 023201 (2006).

[13] N. Zahzam, T. Vogt, M. Mudrich, D. Comparat, and P. Pillet, Phys. Rev. Lett. **96**, 023202 (2006).

[14] W. Ketterle, K. B. Davis, M. A. Joffe, A. Martin, and D. E. Pritchard, Phys. Rev. Lett. **70**, 2253 (1993).

[15] Y. Huang, J. Qi, H. K. Pechkis, D. Wang, E. E. Eyler, P. L. Gould, and W. C. Stwalley, J. Phys. B **39**, S857 (2006).

[16] D. Comparat, C. Drag, B. Laburthe Tolra, A. Fioretti, P. Pillet, A. Crubellier, O. Dulieu, and F. Masnou-Seeuws, Eur. Phys. J. D **11**, 59 (2000).

[17] J. M. Sage, S. Sainis, T. Bergeman, and D. DeMille, Phys. Rev. Lett. **94**, 203001 (2005).

[18] A. Fioretti, C. Amiot, C. M. Dion, O. Dulieu, M. Mazzoni, G. Smirne, and C. Gabbanini, Eur. Phys. J. D **15**, 189 (2001).

[19] M. G. Raizen, R. J. Thompson, R. J. Brecha, H. J. Kimble, and H. J. Carmichael, Phys. Rev. Lett. **63**, 240 (1989).

[20] R. J. Thompson, G. Rempe, and H. J. Kimble, Phys. Rev. Lett. **68**, 1132 (1992).

[21] H. Konishi, K. Roux, V. Helson, and J.-P. Brantut, Nature (London) **596**, 509 (2021).

[22] T. Ray, A. Sharma, S. Jyothi, and S. A. Rangwala, Phys. Rev. A **87**, 033832 (2013).

[23] M. Niranjan, S. Dutta, T. Ray, and S. A. Rangwala, Phys. Rev. A **99**, 033617 (2019).

[24] S. P. Dinesh, V. I. Thakar, V. R. Gokul, A. Bahuleyan, and S. A. Rangwala, EPJ Tech. Instrum. **11**, 1 (2024).

[25] J. J. Sanchez-Mondragon, N. B. Narozhny, and J. H. Eberly, Phys. Rev. Lett. **51**, 550 (1983).

[26] J. J. Childs, K. An, M. S. Otteson, R. R. Dasari, and M. S. Feld, Phys. Rev. Lett. **77**, 2901 (1996).

[27] G. S. Agarwal, Phys. Rev. Lett. **53**, 1732 (1984).

[28] Y. Zhu, D. J. Gauthier, S. E. Morin, Q. Wu, H. J. Carmichael, and T. W. Mossberg, Phys. Rev. Lett. **64**, 2499 (1990).

[29] S. Dutta and S. A. Rangwala, Phys. Rev. A **94**, 053841 (2016).

[30] A.-R. Allouche and M. Aubert-Frécon, J. Chem. Phys. **136**, 114302 (2012).

[31] S. Jyothi, T. Ray, S. Dutta, A. R. Allouche, R. Vexiau, O. Dulieu, and S. A. Rangwala, Phys. Rev. Lett. **117**, 213002 (2016).

[32] R. A. Cline, J. D. Miller, and D. J. Heinzen, Phys. Rev. Lett. **73**, 632 (1994).

[33] W. C. Stwalley and H. Wang, J. Mol. Spectrosc. **195**, 194 (1999).

[34] S. Jyothi, T. Ray, N. B. Ram, and S. A. Rangwala, *Hybrid Ion, Atom, and Light Trap: Ion Traps for Tomorrow's Applications* (Institute of Physics, University of Reading, Berkshire, 2015), pp. 269–287.

[35] J. L. Bohn and P. S. Julienne, Phys. Rev. A **60**, 414 (1999).

[36] C. Drag, B. Tolra, O. Dulieu, D. Comparat, M. Vatasescu, S. Boussen, S. Guibal, A. Crubellier, and P. Pillet, IEEE J. Quantum Electron. **36**, 1378 (2000).

[37] U. Schlöder, C. Silber, T. Deuschle, and C. Zimmermann, Phys. Rev. A **66**, 061403(R) (2002).

[38] J. Léonard, M. Walhout, A. P. Mosk, T. Müller, M. Leduc, and C. Cohen-Tannoudji, Phys. Rev. Lett. **91**, 073203 (2003).

[39] D. S. Weiss, E. Riis, Y. Shevy, P. J. Ungar, and S. Chu, J. Opt. Soc. Am. B **6**, 2072 (1989).

[40] J. Zeiher, J. Wolf, J. A. Isaacs, J. Kohler, and D. M. Stamper-Kurn, Phys. Rev. X **11**, 041017 (2021).

[41] R. Sawant, O. Dulieu, and S. A. Rangwala, Phys. Rev. A **97**, 063405 (2018).

[42] M. Zhu, Y.-C. Wei, and C.-L. Hung, Phys. Rev. A **102**, 023716 (2020).

[43] J. Schnabel, T. Kampschulte, S. Rupp, J. Hecker Denschlag, and A. Köhn, Phys. Rev. A **103**, 022820 (2021).

[44] D. A. Anderson, S. A. Miller, and G. Raithel, Phys. Rev. Lett. **112**, 163201 (2014).

[45] R. Sawant and S. A. Rangwala, Phys. Rev. A **93**, 023806 (2016).

[46] J. Gripp, S. L. Mielke, L. A. Orozco, and H. J. Carmichael, Phys. Rev. A **54**, R3746 (1996).

[47] D. Hoffmann, P. Feng, and T. Walker, J. Opt. Soc. Am. B **11**, 712 (1994).